Structural, optical, and magnetic characterization of monodisperse Fe-doped ZnO nanocrystals

A. Parra-Palomino,[1] O. Perales–Perez,[2,a)] R. Singhal,[1] M. Tomar,[1] Jinwoo Hwang,[3] and P. M. Voyles[3]
[1]*Department of Physics, University of Puerto Rico, Mayagüez, Puerto Rico 00681-9016, USA*
[2]*Department of Engineering Science and Materials, University of Puerto Rico, Mayagüez, Puerto Rico 00681-9044, USA*
[3]*Materials Science and Engineering, University of Wisconsin at Madison, Wisconsin 53706-1595, USA*

(Presented on 6 November 2007; received 11 September 2007; accepted 30 October 2007; published online 14 February 2008)

The results on the synthesis and characterization of highly monodisperse Fe-doped ZnO nanocrystals are presented. Stable suspensions of these materials were produced in an ethanol solution at room temperature. To promote crystal growth, the suspensions of nanocrystals were aged in contact with their mother liquors. X-ray diffraction characterization of doped systems at various Fe-atomic fractions x confirmed the exclusive formation of the host ZnO with the wurtzite structure. High resolution transmission electron microscopy analyses of the suspensions revealed the high monodispersity and crystallinity of the 6–8 nm nanocrystals. Ultraviolet-visible measurements confirmed not only the nanocrystalline nature of the samples but also evidenced the continuous growth of the crystals when aged in their mother liquors. Room-temperature magnetic measurements indicated that the ferromagnetic behavior of doped ZnO was dependent on composition and crystal size of produced nanocrystals. Room-temperature ferromagnetism was established in the nanocrystals synthesized at $x=0.05$ and 0.08 aged for 24 and 360 h, respectively. The corresponding room-temperature coercivity values were 45 and 78 Oe. © *2008 American Institute of Physics*. [DOI: 10.1063/1.2834705]

I. INTRODUCTION

Recent prediction[1,2] on ferromagnetism in wide band gap semiconductors has opened a broad interest in the emergent field of spintronics. It has been found that the diluted magnetic semiconductors can be formed by replacing the cations of III-V or II-VI semiconductors with transition metal ions. Several researchers reported the experimental evidence of ferromagnetism in transition metal-doped ZnO thin film and bulk materials produced by different methods. Abid *et al.*[3] reported ferromagnetic behavior at 3 K with coercivity of 137 Oe in 6% Co-doped ZnO, produced by electrodeposition. Ueda *et al.*[4] deposited $Zn_{1-x}M_xO$ ($x=0.05-0.25$; $M=Co,Mn,Cr,Ni$) films using pulsed laser deposition (PLD) technique. They found that Co-doped ZnO films exhibited ferromagnetism with a Curie temperature (T_C) above 280 K. Ferromagnetism was also observed for Ni-doped ZnO nanocrystals. As-synthesized nanocrystals were paramagnetic, but their aggregation gave rise to robust ferromagnetism.[5,6] Polyakov *et al.*[7] observed room-temperature ferromagnetism in Fe- and Cr-implanted bulk ZnO crystals but after annealing at 700 °C. Optical absorption and microcathodoluminescense measurements suggested the actual incorporation of the transition metal ions. Cho *et al.*[8] found ferromagnetic behavior in (Co, Fe)-doped ZnO film grown by reactive magnetron cosputtering, where the effects of a rapid thermal annealing under vacuum lead to an increase in the magnetization and T_C. Wei *et al.*,[9] have deposited Fe-doped ZnO ($Zn_{1-x}Fe_xO$, $x=0-0.07$) films onto $LiNbO_3$ substrate by magnetron sputtering and found that Fe substituted the Zn site in the 2^+ charge state when $x\leqslant 0.04$ leading to a strong ferromagnetism ($T_C\sim 400$ K). A further increase of the dopant atomic fraction up to 0.07 caused the precipitation of magnetite (Fe_3O_4), which was conducive to the increase in the magnetic moment of the material. More recently, Kamakar *et al.*,[10] produced nanocrystalline Fe-doped ZnO powders by a chemical pyrophoric reaction method. Magnetization measurements suggested the ferromagnetic to paramagnetic transition temperature to be above 450 K. On the other hand, Mandal *et al.*[11] found that the formation of a secondary phase in Fe and other transition metal ion-doped ZnO powders was dependent on the level of doping and sample preparation temperature. On this basis, the present work addressed the room-temperature synthesis of highly monodisperse Fe-doped ZnO nanocrystals in ethanol. The structural, optical, and magnetic characterizations of the synthesized nanocrystals are also presented.

II. EXPERIMENTAL

A. Materials

Zinc acetate, Fe(II) acetate, LiOH, and anhydrous ethanol were of analytical grade and used without further purification. Suitable amounts of Zn and Fe acetate salts were dissolved in ethanol to produce a 0.01*M* solution. A LiOH ethanol solution was the precipitant agent. *n*-heptane was used to coagulate nanocrystals from their suspensions.

a)Electronic mail: ojuan@uprm.edu. Phone: (787)832-4040 x3071. FAX: (787)265-3816.

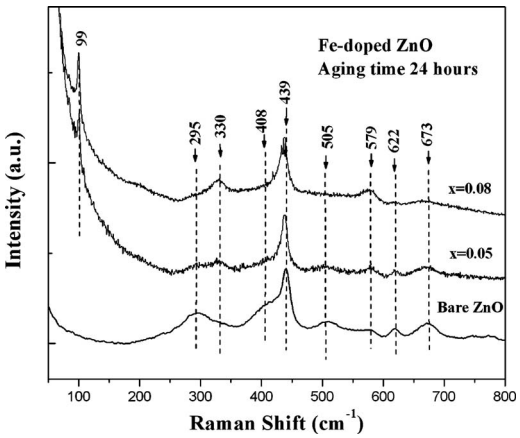

FIG. 1. Raman shift of bare and Fe-doped ZnO nanocrystals synthesized at different atomic fractions of dopant, "*x*."

B. Synthesis of nanocrystals

Doped ZnO nanocrystals were synthesized in ethanol as reported by Spanhel and Anderson for bare ZnO.[12] In our case, the syntheses were carried out under ambient-temperature conditions. Metal ions solutions were prepared for a specific dopant atomic fraction, "*x*." The metals and the hydroxide ethanol solutions were mixed under vigorous stirring for 10 min, followed by their aging at room temperature. Nanocrystals were recovered by successive coagulation/dispersion cycles using *n*-heptane/fresh ethanol and submitted for characterization.

C. Characterization

Powders were characterized by x-ray diffraction (XRD) in a Siemens D5000 diffractometer. Raman studies were performed using Jobin-Yvon T64000 spectrophotometer. A Phillips CM200 high resolution transmission electron microscope (HRTEM) was used to study the crystal structure, morphology, and qualitative composition of the nanocrystals. Ultraviolet-visible (UV-Vis) studies were carried out using a Beckman Coulter DU800 spectrophotometer. *M-H* loops were measured in a Quantum Design MPMS XL-7 superconducting quantum interference device (SQUID) magnetometer.

III. RESULTS AND DISCUSSION

A. XRD diffraction analyses

All XRD peaks of Fe-doped ZnO nanocrystals synthesized at different "*x*" values and different aging times corresponded to ZnO with the wurtzite structure. The absence of any extra peak in these patterns suggests the actual incorporation of dopant into the host oxide structure. An aging of 24 h was necessary to complete the development of the oxide structure for "*x*" values as high as 0.08. The average crystallite size, estimated by using the Scherrer's equation, was around 4.5 nm. The crystallite size was increased by prolonging the aging period (120 and 360 h for a concentration of 5% and 8% of iron, respectively); the corresponding values varied between 6.5 and 8.3 nm.

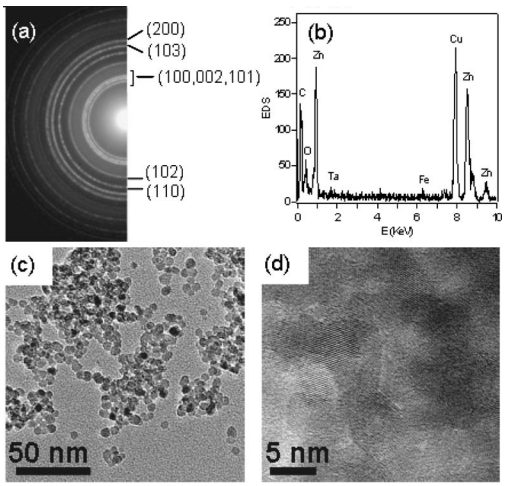

FIG. 2. ED pattern (a), EDS spectrum (b), and HRTEM images [(c) and (d)], of Fe–ZnO nanocrystals ($x=0.08$) aged for 15 days.

B. Raman spectroscopy

Figure 1 shows the Raman spectra of $Zn_{1-x}Fe_xO$ ($x=0.0, 0.05, 0.08$) nanocrystals. The phonon modes at 99.5 and 439 cm^{-1} are assigned to E_2 (low) and E_2 (high) vibrational modes, respectively, and are similar as reported for standard ZnO.[13] As the concentration of Fe increases from 5% to 8%, the ZnO phonon mode shifted to lower frequencies. It may be due to the decrease in binding energy of Zn–O bond as a result of substitution of Zn^{2+} by Fe^{2+}. The frequencies of other fundamental optical modes in the Fe-doped ZnO were E_1 (TO)$=408$ cm^{-1} and A_1 (LO) $=579$ cm^{-1}. The intensity of the later mode was enhanced with a rise in the concentration of dopant. These modes were also reported by Wang *et al.*[14] The phonon mode at 330 cm^{-1} is due to a second order spectral feature originated from the zone-boundary phonons of 2-E_2 (M) for ZnO.[15] The intensity of the Raman modes located at 295, 505, 622, and 673 cm^{-1} decreased with a rise in the concentration of the dopant. The reasons behind this trend are currently under investigation and will be a matter of a forthcoming publication.

C. HRTEM analyses

Figures 2(a) and 2(b) show, respectively, the electron diffraction (ED) and the energy dispersive x-ray spectroscopy (EDS) patterns of Fe–ZnO nanocrystals ($x=0.08$) aged for 15 days. All crystallographic planes in the selected-area ED pattern agreed well with those for ZnO, indicating that the Fe-doped ZnO particles have good crystallinity. No secondary phases were detected. The Cu and Ta signals in the EDS are an artifact from either the TEM grid or the sample area of the TEM (pole pieces, sample rod, etc). HRTEM images of the same nanocrystals are shown in Figs. 2(c) and 2(d). The nanocrystals were highly monodisperse, with a diameter averaging 6 nm. Adsorbed acetate species would have contributed to the establishment of a net surface charge onto the nanocrystals preventing their aggregation.[5]

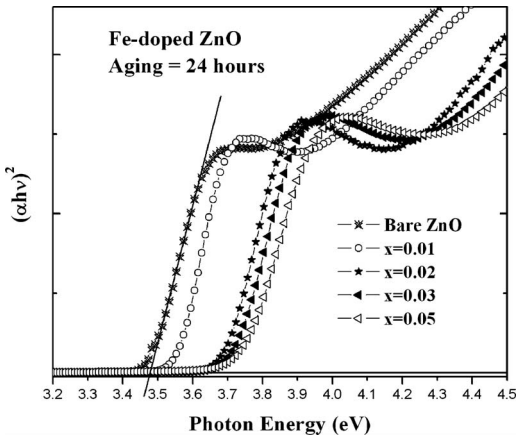

FIG. 3. UV-Vis absorption spectra for nanocrystals synthesized at different atomic fractions of dopant, "*x*," and aged for 24 h.

D. UV-Vis measurements

UV-Vis absorption spectra were recorded from stable transparent suspensions of 24 h aged Fe-doped ZnO nanocrystals (Fig. 3). The optical band gap was obtained by extrapolating of the linear part until it intersects the *X* axis. The band edge and the exciton energy shifted to the blue as the concentration of dopant increased from 1% to 5%. The band gap energy for a concentration of 5% of Fe was estimated at 3.74 eV (335 nm), which is 0.34 eV higher than that for bare ZnO (3.4 eV) produced at the same aging time. This blueshift can be attributed to the quantum confinement effect in the nanocrystals.[16] In turn, the rise in the band gap energy values by increasing "*x*" may suggest the inhibition of crystal growth by the incorporation of dopant species. This trend is in good agreement with our size estimations from XRD measurements of doped ZnO nanocrystals. In addition to crystal size effect, the variation in the band gap energy can also be caused by the dopant incorporation itself. The dependence of band gap energy with dopant concentration has been observed for Fe and Co-doped ZnO (Refs. 17 and 18) films. Although the corresponding results were explained in terms of the distortion of the host lattice and generation of defects, these factors would not play a main role in the determination of the band gap energy because of the negligible variation of the lattice dimensions.[19] Accordingly, the widening in band gap can more likely be attributed to the *sp-d* exchange interaction between band electrons and the localized *d* electrons of Fe substituting Zn ions.

E. SQUID measurements

Figures 4(a) and 4(b), show the room-temperature (RT) *M-H* hysteresis loops for Fe-doped ZnO nanocrystals ($x=0.05,0.08$) aged for 24 and 360 h. Both samples exhibited a small but evident hysteresis with a coercivity of 45 and 78 Oe, and a remnant magnetization of $\sim 2.7\times10^{-5}$ and 4.3×10^{-5} emu g^{-1}, respectively. The formation of magnetite from starting Fe(II) species could be ruled out under the reducing conditions (provided by ethanol) in our system. Moreover, no second phases were detected in HRTEM analyses. Our results are in good agreement with those reported for other ferromagnetic ZnO quantum dots.[5,6] The generation of lattice defects in ZnO and/or lattice distortions due to the incorporation of dopant species could be involved with the observed ferromagnetism.[2,20]

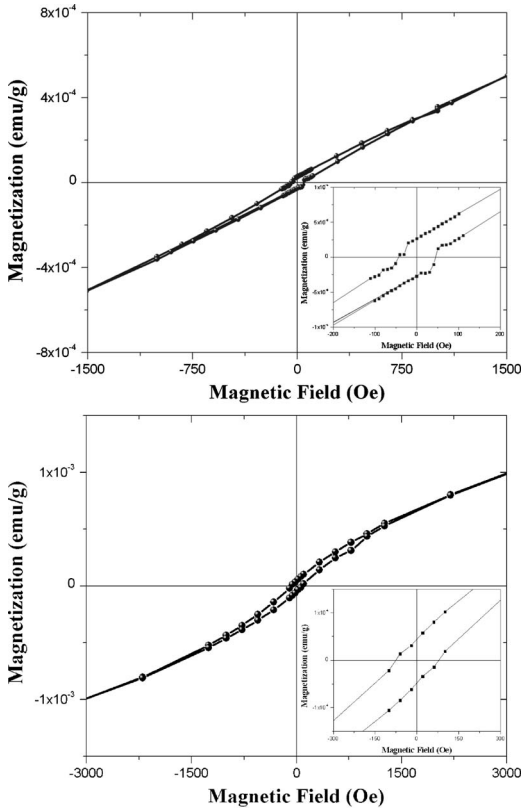

FIG. 4. Room-temperature *M-H* hysteresis loops for Fe-doped ZnO nanocrystals, $x=0.05$, 24 h aged (a), and $x=0.08$, 15 days aged (b).

ACKNOWLEDGMENTS

This material is based upon work supported by the National Science Foundation under PREM (Grant Nos. 0351449 -UPRM and 0304479-UW).

[1]K. Sato and H. Katayama–Yoshida, Semicond. Sci. Technol. **17**, 367 (2002).
[2]T. Dietl *et al.*, Phys. Rev. B **63**, 195205 (2001).
[3]M. Abid *et al.*, J. Electrochem. Soc. **153**, D138 (2006).
[4]K. Ueda *et al.*, Appl. Phys. Lett. **79**, 988 (2001).
[5]O. Perales–Perez *et al.*, Nanotechnology **18**, 315606 (2007).
[6]P. Radovanovic and D. Gamelin, Phys. Rev. Lett. **91**, 157202 (2003).
[7]A. Y. Polyakov *et al.*, Mater. Sci. Semicond. Process. **7**, 77 (2004).
[8]Y. M. Cho *et al.*, Appl. Phys. Lett. **80**, 3358 (2002).
[9]X. X. Wei *et al.*, J. Phys.: Condens. Matter **18**, 7471 (2006).
[10]D. Karmakar *et al.*, Phys. Rev. B **75**, 144404 (2007).
[11]S. K. Mandal *et al.*, Appl. Phys. Lett. **89**, 144105 (2006).
[12]L. Spanhel and M. A. Anderson, J. Am. Chem. Soc. **113**, 2826 (1991).
[13]J. Serrano *et al.*, Phys. Rev. B **69**, 094306 (2004).
[14]X. B. Wang *et al.*, J. Phys. D **39**, 4992 (2006).
[15]J. M. Calleja and M. Cardona, Phys. Rev. B **16**, 3753 (1977).
[16]N. S. Norberg *et al.*, J. Am. Chem. Soc. **126**, 9387 (2004).
[17]Y. Z. Peng *et al.*, J. Supercond. **18**, 97 (2005).
[18]A. J. Chen *et al.*, J. Phys. D **39**, 4762 (2006).
[19]Z. W. Zhao *et al.*, Appl. Phys. Lett. **90**, 152502 (2007).
[20]C. Song *et al.*, J. Phys.: Condens. Matter **19**, 176229 (2007).